Supporting Information

Floating Zone Crystal Growth, Structure, and Properties of a Cubic $Li_{5.5}La_3Nb_{1.5}Zr_{0.5}O_{12}$ Garnet-Type Lithium-Ion Conductor

Caleb Ramette[a], Lucas Pressley[b,c,†], Maxim Avdeev[d,e], Minseong Lee[f], Satya Kushwaha[b,g], Matthew Krogstad[h], Suchismita Sarker[i], Paul Cardon[a], Jacob Ruff[i], Mojammel Khan[b,g], Kunimitsu Kataoka[j], Tyrel McQueen[b,c,g], Huiwen Ji[a,*]

[a]Department of Materials Science & Engineering, University of Utah, Salt Lake City, Utah 84112, USA

[b]Department of Chemistry, The Johns Hopkins University, Baltimore, Maryland, 21218, USA

[c]Department of Materials Science and Engineering, The Johns Hopkins University, Baltimore, Maryland, 21218, USA

[d]Australian Centre for Neutron Scattering, Australian Nuclear Science and Technology Organisation (ANSTO), New Illawarra Rd, Lucas Heights NSW 2234, Sydney, Australia

[e]School of Chemistry, University of Sydney, NSW, 2006, Sydney, Australia

[f]National High Magnetic Field Laboratory, Los Alamos National Laboratory, Los Alamos, New Mexico 87545, USA

[g]Platform for the Accelerated Realization, Analysis and Discovery of Interface Materials (PARADIM), Department of Chemistry, The Johns Hopkins University, Baltimore, Maryland, 21218, USA

[h]Argonne National Laboratory, Materials Science Division, 9700 S. Cass Avenue, Lemont, IL 60439, USA

[i]CHESS, Cornell University, Ithaca, NY, 14853, United States

[j]National Institute of Advanced Industrial Science and Technology, AIST Tsukuba Centre 5, Japan

[*]Corresponding author: huiwen.ji@utah.edu

[†]Present address: Oak Ridge National Laboratory, Oak Ridge, TN 37830, USA

Table of Contents:

Supplementary Figure S1 – Quartz sample chamber before and after HPFZ crystal growth

Supplementary Figure S2 – Counter- and parallel-rotated Li5.5-LLNZO rod segments

Supplementary Figure S3 – Bank 2 powder XRD pattern for Li5.5-LLNZO

Supplementary Figure S4 – Bank 3 powder XRD pattern for Li5.5-LLNZO

Supplementary Figure S5 – Scanning electron microscopy (SEM) image of polished surface of Li5.5-LLNZO single crystal plate

Supplementary Figure S6 – XRD in Bragg-Brentano geometry of polished Li5.5-LLNZO single crystal plate

Supplementary Table S1 – Crystal structure refinement from neutron Laue single-crystal diffraction

Supplementary Figure S7 – DC polarization measurements of Li5.5-LLNZO single crystal plate

Supplementary Figure S8 – Dielectric constant as a function of frequency from 3-400 K

Supplementary Figure S9 – Dielectric loss tangent (δ) as a function of frequency

from 3-400 K

Supplementary Figure S1 – Quartz sample chamber before and after HPFZ crystal growth

The quartz sample chamber before (left) and after (right) crystal growth shows the cloudy white coating from material evaporation deposited on the inside wall of the quartz tube, which is highly detrimental to light transmission through the sample chamber to the focal point at the molten zone.

Supplementary Figure S2 – Counter- and parallel-rotated Li5.5-LLNZO rod segments

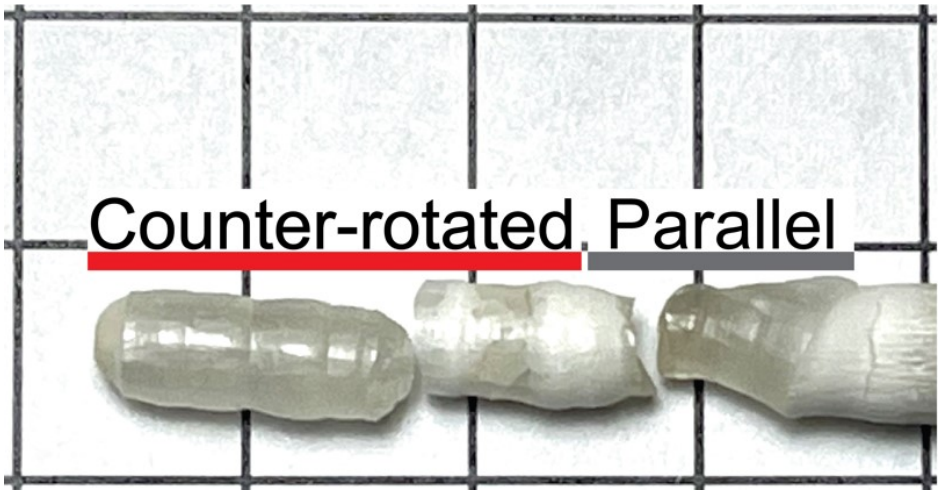

Li5.5-LLNZO rod segments synthesized with counter-rotation (left) and parallel-rotation (right) indicated with red and grey labelling, respectively. Background grid indicates 1 cm lengths. The 10 mm single crystal region imaged in Figure 1c and d that was used for structural, electrochemical, and dielectric studies is the single, cohesive segment on the left end of the crystal boule in this image. While the crystal rod cracked during transit, fracturing occurred along domain boundaries.

Supplementary Figure S3 – Bank 2 powder XRD pattern for Li5.5-LLNZO

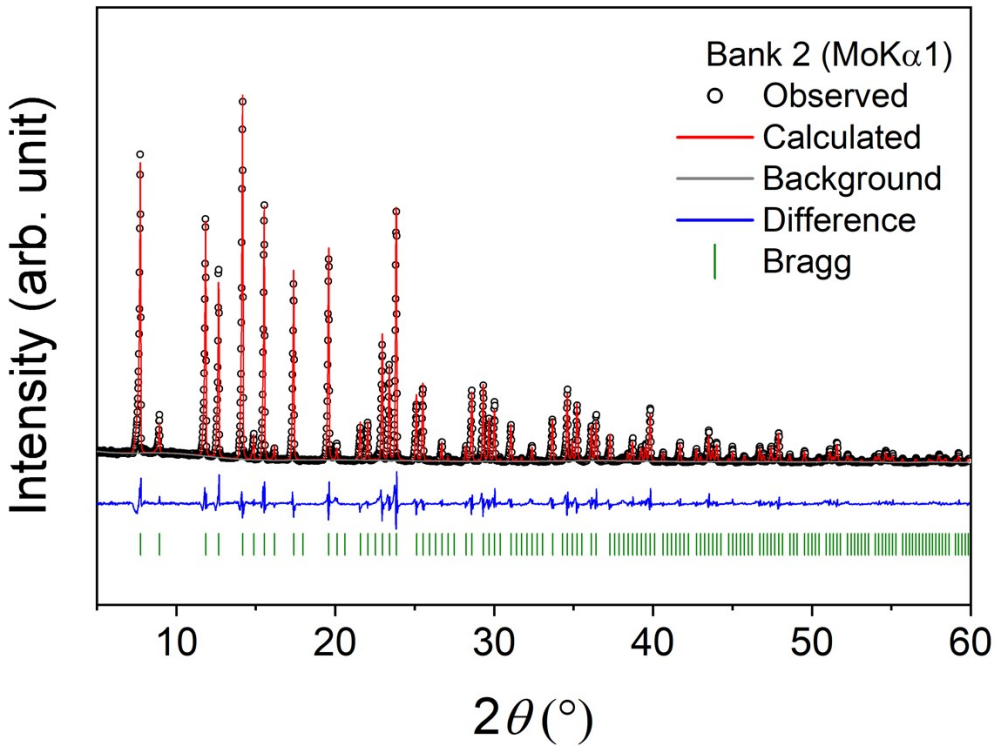

Experimental data are shown as black circles, calculated pattern in red, difference profile in blue, and calculated Bragg reflection positions in green.

Supplementary Figure S4 – Bank 3 powder XRD pattern for Li5.5-LLNZO

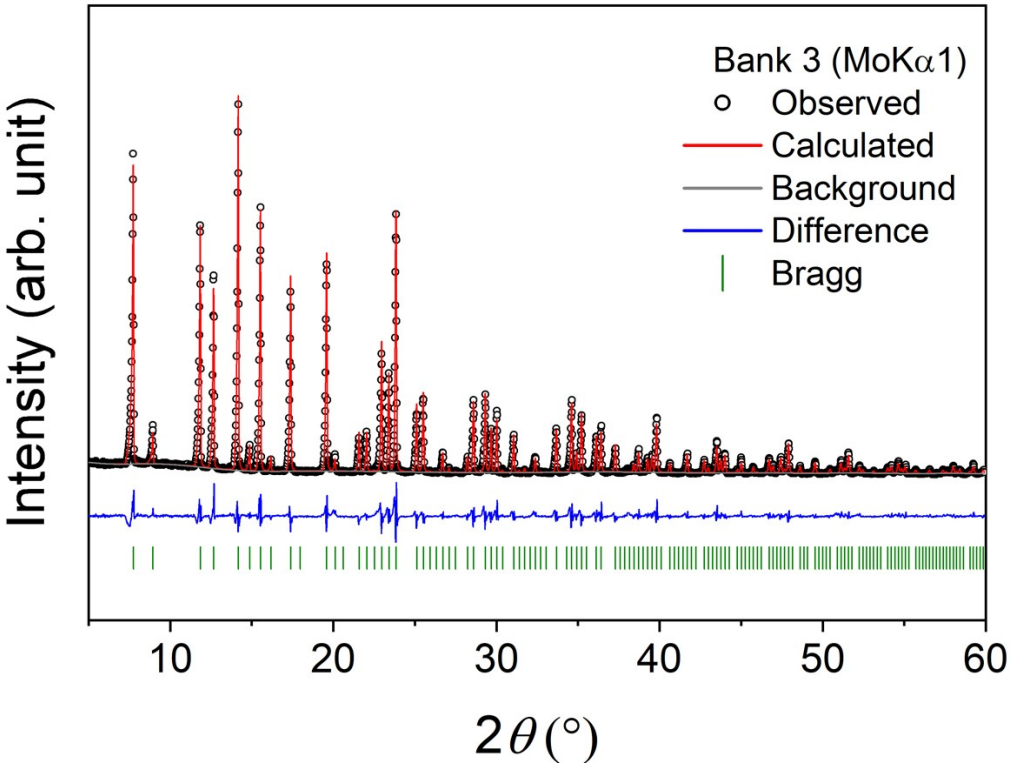

Experimental data are shown as black circles, calculated pattern in red, difference profile in blue, and calculated Bragg reflection positions in green.

Supplementary Figure S5 – Scanning electron microscopy (SEM) image of polished surface of Li5.5-LLNZO single crystal plate

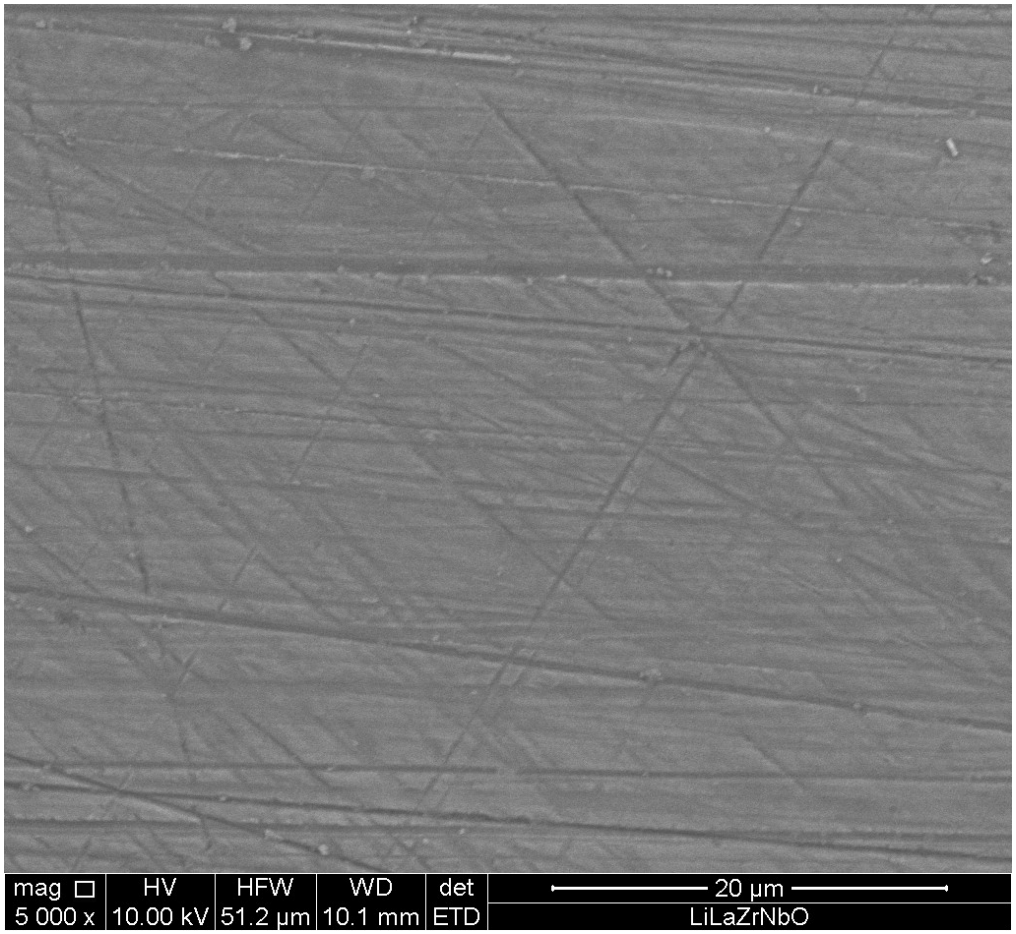

Supplementary Figure S6 – XRD in Bragg-Brentano geometry of polished Li5.5-LLNZO single crystal plate

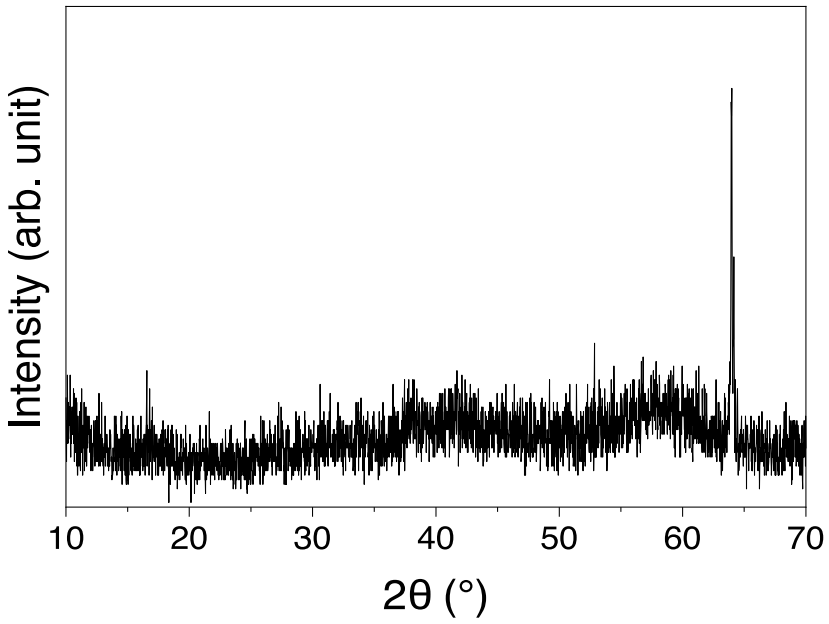

The peak was identified as the (752) peak from comparison with the average structure determined by powder XRD performed on a ground single crystal segment (see Fig. S4).

Supplementary Table S1 – Crystal structure refinement from neutron Laue single-crystal diffraction

Refined composition	$Li_{5.60(11)}La_3Nb_{0.75}Zr_{0.25}O_{12}$
Cell parameter, a (Å)*	12.83406
Cell volume, V ($Å^3$)*	2113.94
Z	8
Density (g/cm^3)	5.26
Reflections	1116
Reflections >3s	491
Parameters	26
R, I > 3s	0.0460
wR, I > 3s	0.0501
Goodness of fit	1.22

* Determined from X-ray powder diffraction data collected for ground crystal

Supplementary Figure S7 – DC polarization measurements of Li5.5-LLNZO single crystal plate

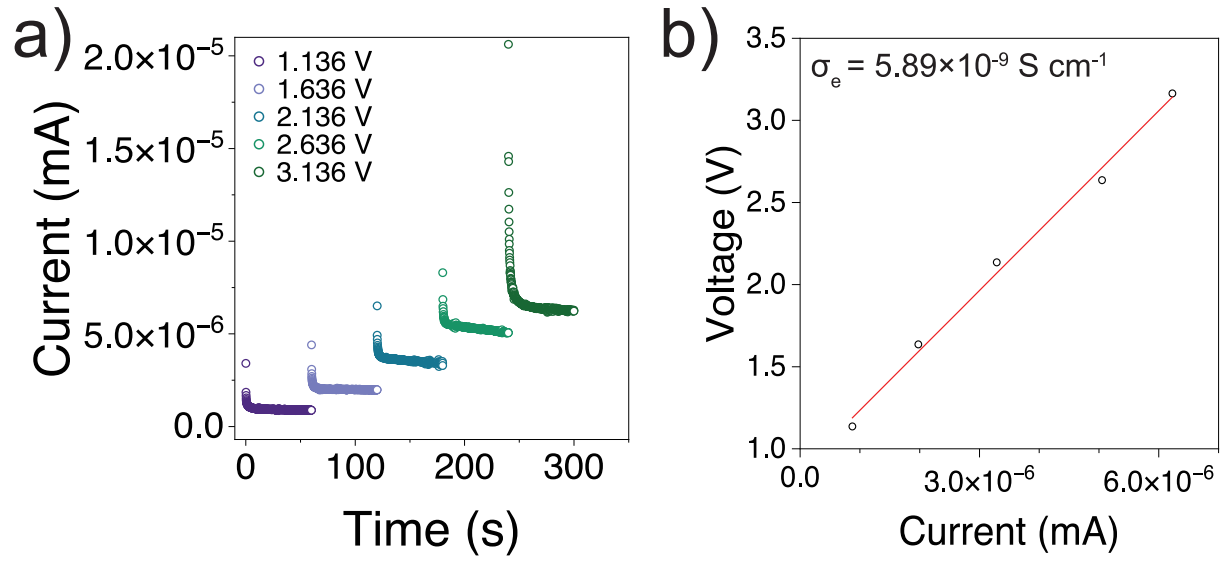

Final steady current values from the d.c. polarization curves measured over a range of voltages in a) were used in calculating the electronic conductivity from the linear fitting based on Ohm's Law shown in b) (R^2=0.993).

Supplementary Figure S8 – Dielectric constant as a function of frequency from 3-400 K

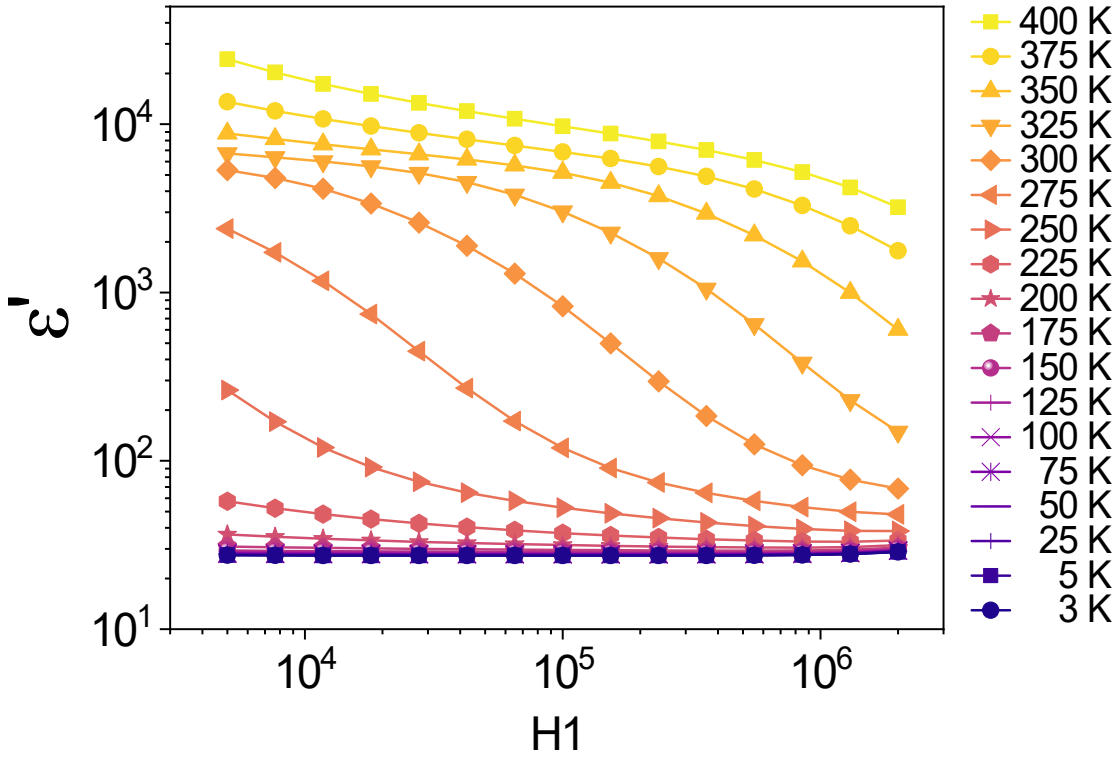

Supplementary Figure S9 – Dielectric loss tangent (δ) as a function of frequency from 3-400 K